DOI:10.1021/jf1007659

JOURNAL OF AGRICULTURAL AND FOOD CHEMISTRY
ARTICLE

Nanobiocomposites of Carrageenan, Zein, and Mica of Interest in Food Packaging and Coating Applications

Maria D. Sanchez-Garcia,[†] Loic Hilliou,[‡,§] and Jose M. Lagaron*,[†]

[†]Novel Materials and Nanotechnology Group, Instituto de Agroquímica y Tecnología de Alimentos (IATA), Consejo Superior de Investigaciones Científicas (CSIC), Av. Agustin Escardino 7, 46980 Paterna, Spain, [‡]Institute for Nanostructures, Nanomodelling and Nanofabrication (I3N), University of Minho, 4800-048 Guimaraes, Portugal, and [§]REQUIMTE, Faculty of Engineering, University of Porto, Rua Dr. Roberto Frias s/n, 4200-465 Porto, Portugal

The present study presents the development and characterization of biocomposites of a red-algae-derived carrageenan, mica, and their blends with zein prolamine obtained by solvent casting. The morphology of the blends was characterized by scanning and transmission electron microscopy (SEM and TEM), optical microscopy, and atomic force microscopy (AFM). Mechanical behavior, water barrier, water uptake, and UV−vis protection of the cast films were also investigated. The results indicated that the addition of 10 wt % glycerol to the blends resulted in a better dispersion of the additive and, for that reason, a better improvement for the studied properties. The composites were seen colored but transparent and exhibited the ability to block the UV−vis radiation because of the characteristic absorbing properties of the filler. Nevertheless, the main conclusion from the work is that the nanocomposites were seen to act as a reinforcing plasticizer and also led to significantly reduced water permeability and uptake. The clay was found to be more efficient in the latter aspect than the zein prolamine as an additive. As a result, these novel carragenan-based biocomposites can have significant potential to develop packaging films and coatings for shelf-life extension of food products.

KEYWORDS: Carrageenan; food hydrocolloids; nanocomposites; packaging; coatings

1. INTRODUCTION

Biopolymer films have been the focus of worldwide attention for the past few decades because they offer favorable environmental advantages in terms of sustainability and compostability compared to conventional synthetic polymeric films. Edible and biodegradable natural polymer films offer alternative packaging with lower environmental costs. The search for new renewable resources for the production of edible and biodegradable packaging materials and coatings has steadily increased in recent years. In particular, nonconventional sources of carbohydrates have been extensively studied. There are various unique carbohydrates that are found in marine organisms that represent a largely unexplored source of valuable materials. These nonconventional and underexploited renewable materials can be used as an interesting alternative to produce edible films and coatings.

The biopolymers studied in this work to produce edible films and coatings were κ/ι-hybrid carrageenan extracted from *Mastocarpus stellatus*, an underexploited red algae present in the Portuguese marine coast (*1*−*4*). Carrageenans are water-soluble polymers with a linear chain of partially sulfated galactans, which present high potentiality as film-forming material. Carrageenans are structural polysaccharides from red seaweed and have been used extensively in foods, cosmetics, and pharmaceuticals (*5*). Carrageenan biopolymer extracted from *M. stellatus* seaweeds was shown to be a κ/ι-hybrid carrageenan (*1*) with gel properties comparable to commercial κ-carrageenan gel formers (*2*, *3*). The use of carrageenan as edible films and coatings is already used in the food industry on fresh and frozen meat, poultry, and fish to prevent superficial dehydration (*6*), ham or sausage casings (*7*), granulation-coated powders, dry solid foods, oily foods (*8*), etc. but also to manufacture soft capsules (*9*, *10*) and, especially, nongelatin capsules (*11*). Polysaccharide and protein film materials are characterized by high moisture permeability, low oxygen and lipid permeability at lower relative humidities, and compromised barrier and mechanical properties at high relative humidities (*12*).

To tailor the properties and improve the water resistance of these biopolymers, it is often desirable to combine with, for instance, other biopolymers more resistant to water or with the addition of nanoclays. In the case of the addition of nanoclays, these layers are known to form impermeable shields. As a consequence, it is expected that the nanocomposite carbohydrate film will have substantially reduced water vapor permeability, thus helping to solve one of the long-standing drawbacks in the use of biopolymer films, i.e., water plasticization (*13*). Indeed, Lagaron et al. (*13*) showed that the dispersion of mica nanoclay layers into the biopolymer matrix greatly improved the overall water barrier without measurable impact in the biodegradability of the matrix, thus turning them into industrially attractive

*To whom correspondence should be addressed. E-mail: lagaron@iata.csic.es.

 Published on Web 05/10/2010

materials. Moreover, the addition of glycerol to carrageenan has permitted us to obtain more usable film forming materials. Plasticizers are very important components to tailor the physicochemical properties of biopolymers. In principle, the addition of plasticizers results in a decrease in the intermolecular forces along the polymer chains, which consequently improve flexibility, extensibility, toughness, and tear resistance of biopolymer films. To enhance the barrier properties of biopolymer films, a high cross-link density has often been promoted. As a result, an increase in the plasticizer concentration normally causes an increase in the water permeability of hygroscopic or hydrophilic films because of a reorganization of the macromolecular network and a subsequent increase in free volume. Indeed, some studies have reported that the addition of plasticizers yield marked increases in permeability and diffusion coefficients of gas or water vapor (*14*, *15*). However, this effect depends upon the glycerol content in the polymer. In fact, it has been reported that a decrease in water permeability takes place for low additions of glycerol, between 5 and 10%, but that increasing the glycerol content increases the water permeability (*16*, *17*).

In this work, carrageenan was also combined with zein, another biopolymer from the group of alcohol-soluble proteins (prolamines) found in the corn endosperm. The film-forming properties of zein have also been recognized for decades and are the basis for most commercial use of zein. Even when zein is a protein, it presents unusually high resistance to water. Zein films are also brittle, and plasticizers are often recommended. Zein-based films show great potential for uses in edible coatings and bio-based packaging (*18*). In a preliminary study, Arora and Padua developed nanocomposites of zein and reported a water vapor permeability decrease of ca. 50% with the addition of kaolinite clays (*19*). In some studies, zein was blended with other proteins, such as gluten (*20*), starch (*21*) and soy protein (*22*). These were reported to exhibit enhanced mechanical performance as a result of blending. Corradini et al. reported a decrease in water uptake with the addition of zein in starch films plasticized with glycerol (*23*).

However, very little is known about the development and characterization of carrageenan nanocomposites. Daniel-Da-Silva et al. reported the production of polysaccharide ι-carrageenan used in the production of macroporous composites containing nano-sized hydroxyapatite, with application in bone tissue engineering (*24*). Gan et al. also reported a new injectable biomaterial carrageenan/nanohydroxyapatite/collagen for bone surgery (*25*). To the best of our knowledge, the addition of nanoclays in pure carrageenan and the study of the barrier properties of these nanocomposites have not yet been reported.

In this context, the overall objective of this work was the development of novel renewable and biodegradable carrageenan-based food packaging films with improved barrier properties, especially with enhanced water and UV-light resistance. To do so, blends of carrageenan extracted from a Portuguese red algae with a water-resistant zein prolamine and/or with nanoclays were developed and characterized for the first time.

2. EXPERIMENTAL PROCEDURES

2.1. Materials. Details about the recovery of κ/ι-hybrid carrageenan biopolymers from *M. stellatus* seaweeds can be found elsewhere (*1*, *2*, *5*). The polysaccharide used in the present study was obtained through a hot extraction process performed for 2 h at 95 °C and a pH of 8 on alkali-treated *M. stellatus* seaweeds. The resulting powder was then purified by mixing 1 g of isolated product with 49 mL of hot distilled water for 1 h and subsequent centrifugation performed at sequence cycles at 10^4 rpm and 40 °C for 40 min. The supernatant was finally recovered and used for film forming by casting.

Zein from corn (grade Z3625) purchased from Sigma-Aldrich (Madrid, Spain) was used as received without further purification. Glycerol was used as a plasticizer and supplied by Panreac Quimica S.A. (Spain).

A food contact complying NanoBioTer grade based on purified natural mica clay was kindly supplied by NanoBioMatters S.L. (Paterna, Spain). No further details of sample preparation and modification were disclosed by the manufacturer.

2.2. Preparation of the Nanocomposites. Solution-cast film samples of the purified carrageenan with 1, 5, 10 and 20 wt % clay and 10 wt % glycerol content were prepared with a dry film thickness of around 50 μm. Nanoclay dispersions in water were simply mixed in a homogenizer (Ultraturrax T25 basic, Ika-Werke, Germany) for 2 min, then stirred with the carrageenan for 30 min, and subsequently, cast onto Petri dishes to generate films of ca. 50 μm after solvent evaporation at room-temperature conditions.

Solution-cast, 50 μm thickness, film samples of the nanocomposites of carrageenan containing 5 wt % clay, 20 wt % zein, and 25 wt % glycerol were also prepared. A solution of zein in water/ethanol (70:30, v/v) was first prepared and then added to a suspension of nanoclays in carrageenan prepared as described above. The solution was then stirred for 30 min and, subsequently, cast onto Petri dishes. The nanocomposites of zein and carrageenan−zein blends were only obtained with 5 wt % clay, because of the fact that the best property balance was found for compositions around or below this loading level.

2.3. Optical Polarized Light Microscopy (PLM). PLM examinations using an ECLIPSE E800-Nikon with a capture camera DXM1200F-Nikon were carried out on both sides of the cast samples.

2.4. Scanning Electron Microscopy (SEM) Measurements. For SEM observation, the samples were criofractured after immersion in liquid nitrogen, mounted on bevel sample holders, and sputtered with Au/Pd in a vacuum. The SEM pictures (Hitachi S4100) were taken with an accelerating voltage of 10 keV on the sample thickness.

2.5. Transmission Electron Microscopy (TEM) Measurements. TEM was performed using a JEOL 1010 equipped with a digital Bioscan (Gatan) image acquisition system. TEM observations were very difficult to perform because of solubility and difficult handling of the films. However, some pictures were taken on microdrops of the solution cast directly onto the TEM observation grids.

2.6. Atomic Force Microscopy (AFM) Measurements. AFM measurements were performed using an Agilent 5500 SPM system (provided by Scientec Iberica, Spain) to investigate the morphology of the nanocomposite surfaces on both sides of the cast films. The images were scanned in tapping mode in air using commercial Si cantilevers, with a resonance frequency of 320 kHz.

2.7. Gravimetric Measurements. Water permeability was determined from the slope of the weight gain−time curves at 24 °C. The films were sandwiched between the aluminum top (open O-ring) and bottom [deposit for the silica gel that provides 0% relative humidity (RH)] parts of a specifically designed permeability cell with screws and placed inside a desiccator at 75% RH. A Viton rubber O-ring was placed between the film and the bottom part of the cell to enhance sealability. The solvent weight gain through the film was monitored and plotted as a function of time. Cells with aluminum films were used as control samples to estimate water gain through the sealing. Solvent permeation rates were estimated from the steady-state permeation slopes. Water vapor weight gain was calculated as the total cell weight gain minus the gain through the sealing. The tests were performed in duplicate.

For the water uptake, samples were dried in a desiccator at 0% RH until a constant weight. They were then allowed to saturate in moisture inside desiccators at 11, 54, and 75% RH and monitored during sorption until a constant weight (indicating water uptake). These experiments were performed in triplicate.

2.8. Tensile Test. The tensile test was measured at 10 mm/min according to American Society for Testing and Material (ASTM) Standard D638 in stamped dogbone-shaped specimens of the samples, using an Instron testing machine (model 4469, Instron Corp., Canton, MA). The tensile tests were carried out at ambient conditions, i.e., typically 21 °C and 60% RH, and the tests were performed in quadruplicate. The samples were preconditioned in a desiccator at 60% RH before testing.

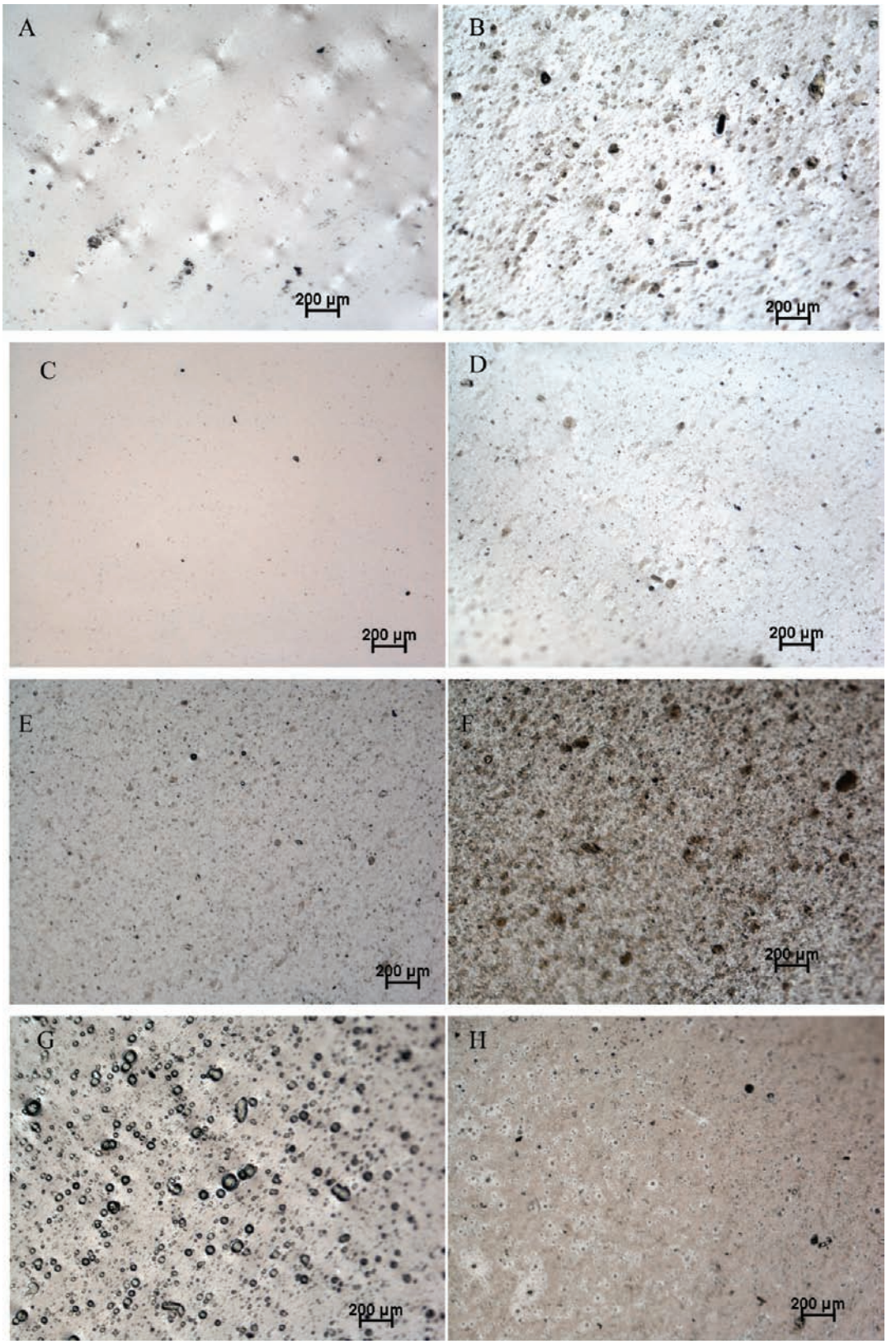

Figure 1. Optical micrographs of (A) carrageenan, (B) carrageenan with 5 wt % clay content, (C) carrageenan with 10 wt % glycerol content, (D) carrageenan with 1 wt % clay content and 10 wt % glycerol content, (E) carrageenan with 5 wt % clay content and 10 wt % glycerol content, (F) carrageenan with 20 wt % clay content and 10 wt % glycerol content, (G) carrageenan with 20 wt % zein content and 10 wt % glycerol content, and (H) carrageenan with 20 wt % zein content, 5 wt % clay content, and 10 wt % glycerol content. The scale marker is 200 μm in all of the micrographs.

2.9. Ultraviolet−Visible (UV−Vis) Spectra. A UV−vis spectrophotometer (Hewlett-Packard 8452A diode array spectropotometer) was used to measure the absorbance and transmittance spectra of the films in the range of 200−700 nm wavelength light. UV−vis spectra were taken in thin films of biodegradable materials, and their nanocomposites were cast directly onto the surface of a quartz cuvette. The measurements were later normalized to an average thickness of 30 μm for all of the samples to allow for a comparison between materials.

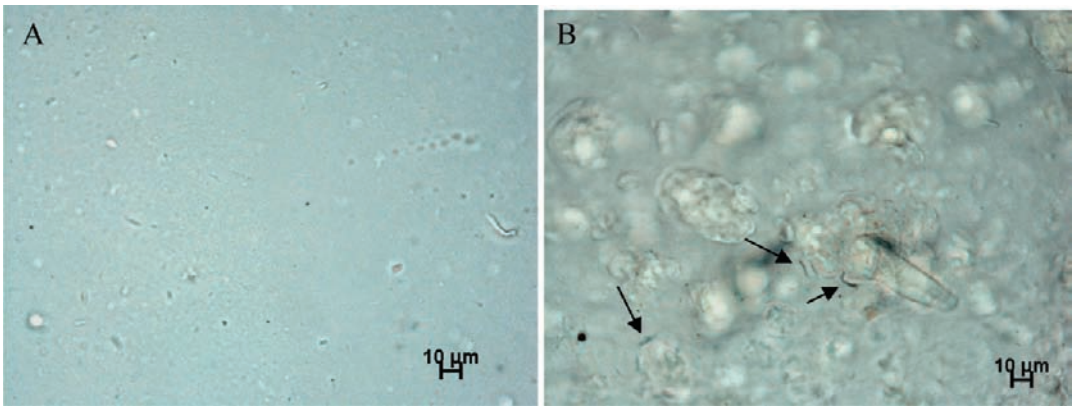

Figure 2. Typical optical micrographs of (A) carrageenan with 10 wt % glycerol content and (B) carrageenan with 5 wt % clay content and 10 wt % glycerol content. The scale marker is 10 μm in the micrographs.

3. RESULTS AND DISCUSSION

3.1. Morphology. Optical PLM photographs were aimed at the characterization of the dispersion of the glycerol phase and the nanoclays in the biodegradable matrixes. **Figure 1** shows the optical micrographs of the carrageenan castings with and without glycerol and with different clay contents. In **Figure 1A**, films of pure carrageenan exhibit some spots, most likely as a consequence of some residues. However, **Figure 1B** indicates that clay tactoids (5 wt %) can be clearly observed in the nonplasticized carrageenan matrix. Panels **C**−**F** of **Figure 1** show micrographs of the carrageenan containing 10 wt % glycerol and 0, 1, 5, and 20 wt % clay content, respectively. A first observation from these images is that an apparent better dispersion of the clay occurs in the presence of glycerol (compare panels **B** and **E** of **Figure 1**). Thus, the presence of glycerol permits us to increase the compatibility and hence dispersion between the clay and the biopolymer in the nanocomposites. From these images, it can also be seen that, with increasing clay content from 1 to 20 wt %, the clay agglomerates (compare panels **D** and **F** of **Figure 1**). Mica has very large platelets, which upon dispersion, even if this is poorer than with other more conventional nanoclays, should provide high shielding efficiency in terms of low-molecular-weight species diffusion (*13*). In principle, this is the reason why it becomes relatively easy to observe big tactoids by optical microscopy because the length and width dimensions of the platelets should tend to naturally seat during film forming parallel to the casting dishes as a result of gravitational and surface energy forces (*26*).

Figure 1G shows a picture taken in the blend of carrageenan containing 20 wt % zein and 10 wt % glycerol. This picture shows a clear phase segregation of most likely the zein phase in the polysaccharide matrix. However, **Figure 1H** shows that the ternary blend is better dispersed in the presence of the nanoclay.

Figure 2 shows a picture with higher magnification taken in a film of carrageenan containing 10 wt % glycerol and 5 wt % clay. From **Figure 2A**, it can be clearly observed that glycerol forms a separate phase at the microscale within the carrageenan matrix, which is very homogeneously dispersed. Curiously, clay platelets are observed to be displayed inside glycerol particles and at the interphase between the glycerol and the matrix (see arrows), suggesting again a higher affinity for the glycerol, which may then act as a compatibilizer for the filler (see **Figure 2B**).

Figure 3 shows the scanning micrographs of the cross-section of these biopolymer blends. For pure carrageenan, a homogeneous film morphology is observed (see **Figure 3A**). In the case of carrageenan with 5 wt % clay content and 10 wt % glycerol (see **Figure 3B**), the presence of the clay cannot be discerned. However, from **Figure 3C**, it can be seen that, in the carrageenan−zein blend, which phase-separates, there seems to be a strong interfacial adhesion between the biopolymer matrix and the protein. The two polymers are, therefore, not miscible but compatible because of the observed interfacial contact. A similar morphology is also observed for the nanocomposite of the carrageenan−zein blend (see **Figure 3D**). **Figure 3E** shows the morphology of pure zein with analogous morphology as the zein composites with clay, suggesting a fine dispersion and adhesion of the nanoclay in the zein matrix (see **Figure 3F**).

Figure 4 shows some TEM results taken on specimens of plasticized carrageenan containing 5 wt % nanoclay. This figure indicates a highly dispersed irregular morphology consisting of intercalated tactoids with thickness in the nano-range, i.e., below 100 nm, and some exfoliated nanoclay platelets most likely fractured.

Finally, **Figure 5** shows the surface roughness of a carrageenan cast film containing 5 wt % nanoclay content and 10 wt % glycerol as measured by AFM. From observation of this figure, it can be seen that the nanoclay contains large platelets strongly intercalated and dispersed at the nanolevel but not to an individual platelet level, which would have meant exfoliation, across the matrix. This figure also shows that there appears to be a good adhesion of the nanofiller to the biopolymer.

3.2. Mechanical Properties. Specimens of carrageenan, zein, and blends of carrageenan−zein and their nanocomposites with glycerol were measured in tensile testing experiments to evaluate the effect of adding nanoclays and zein on the mechanical properties of these biopolymers. Mechanical parameters, such as tensile strength, Young's modulus, and elongation at failure, are presented in **Figure 6**. **Figure 6** shows that the stiffness, strength, toughness, as well as the elongation at failure have a general trend of increasing in the materials with an increasing clay content in the materials. This suggests a reinforcing plasticizer effect of the nanoclay in the material, which in turn allows for better mechanical handling of the films.

In **Figure 6A**, the tensile strength carrageenan is seen to increase with the nanoclay content; this behavior has been reported in different studies with nanoclays (*27*, *28*). This suggests that the nanoclays act to reinforce the material as expected. The addition of nanoclays to carrageenan resulted in an increase in the tensile strength of ca. 39 and 146% for the films of carrageenan with 10 and 20 wt % nanoclay, respectively, compared to carrageenan containing 1 wt % filler content. Nanocomposites with 1 wt % filler are referenced because pure carragenan films could not be tensile tested even with 10 wt % glycerol because of excessive fragility. This was expected because earlier studies (*2*−*4*) reported Young's modulus as low as 25 MPa and a strain at break as low as

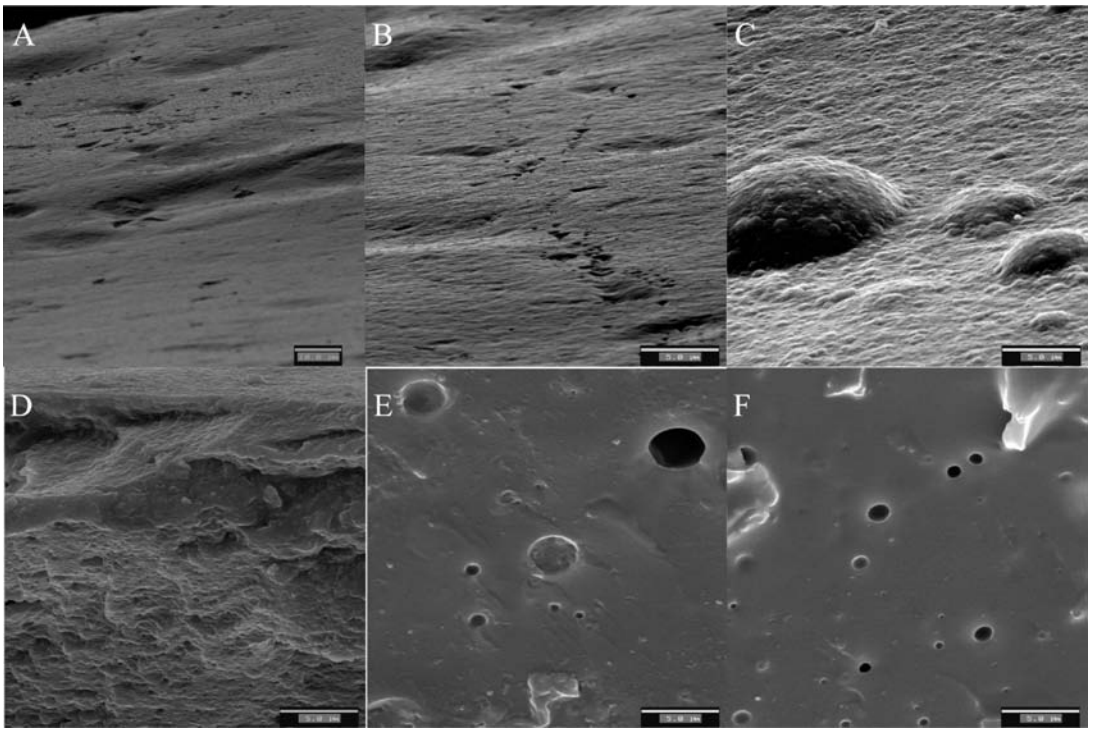

Figure 3. Scanning electron micrographs of the cross-section of (A) carrageenan (scale marker is 10 μm), (B) carrageenan with 5 wt % clay content and 10 wt % glycerol content (scale marker is 5 μm), (C) carrageenan with 20 wt % zein content and 10 wt % glycerol content (scale marker is 5 μm), (D) carrageenan with 5 wt % clay content, 20 wt % zein content, and 10 wt % glycerol content (scale marker is 5 μm), (E) zein with 10 wt % glycerol content, and (F) zein with 5 wt % clay content and 10 wt % glycerol content (scale marker is 5 μm).

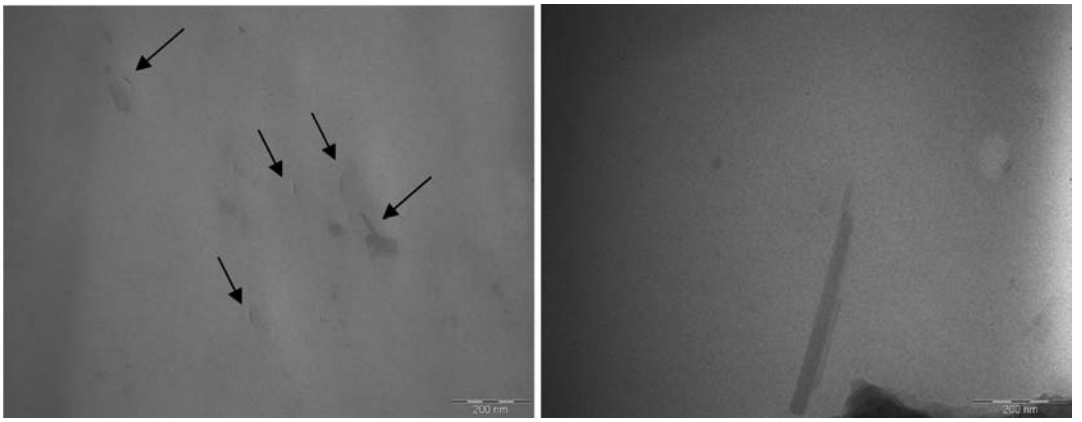

Figure 4. Transmission electron micrographs of plasticized carrageenan containing 5 wt % clay (scale marker is 200 nm).

3.5% for a pure carrageenan film. The increase in tensile strength with a further addition of clay is attributed to a good nanoclay dispersion of these nanocomposites. This behavior is in contrast with the work by Majdzadeh-Ardakani et al., who reported that the addition of high nanoclay loadings into the starch matrix led to the appearance of clay stacks, non-exfoliated morphologies, and even aggregates that deteriorated the mechanical properties and decreased the tensile strength of the higher loaded specimens (*29*). Curiously, in zein cast films, albeit the error bars are relatively high, the tensile strength appeared to decrease in the film with 5 wt % nanoclay compared to the pure zein, most likely because of the poorer morphology of the nanocomposites with zein.

The addition of zein to the carrageenan films increased the tensile strength by up to 72% compared to the carrageenan matrix. Kim et al. reported an analogous behavior; i.e., the addition of zein to gluten increased the mechanical properties until the content of zein reached 20−22%. A further increase in zein content lowered the mechanical properties (*20*). Pol et al. also showed that the tensile strength of soy protein laminate films increased (within a 95% confidence level) with the increasing relative content of zein in the laminates (*22*).

Nanocomposites of the blends of carrageenan−zein seemed to exhibit similar tensile strength, albeit the error bar is relatively high, but carragenan improved this property with the addition of zein, at least compared to the nanocomposite of carrageenan with 1 wt %.

Young's modulus, expressing the stiffness of the material, showed a general trend of increasing values in the nanocomposites, albeit this was not seen for some samples. **Figure 6B** shows Young's modulus of these biopolymers as a function of the nanoclay content. Young's modulus generally increased in carragenan with an increasing clay content, in line with the typical behavior in nanocomposites (*30*, *31*). Thus, an increase in

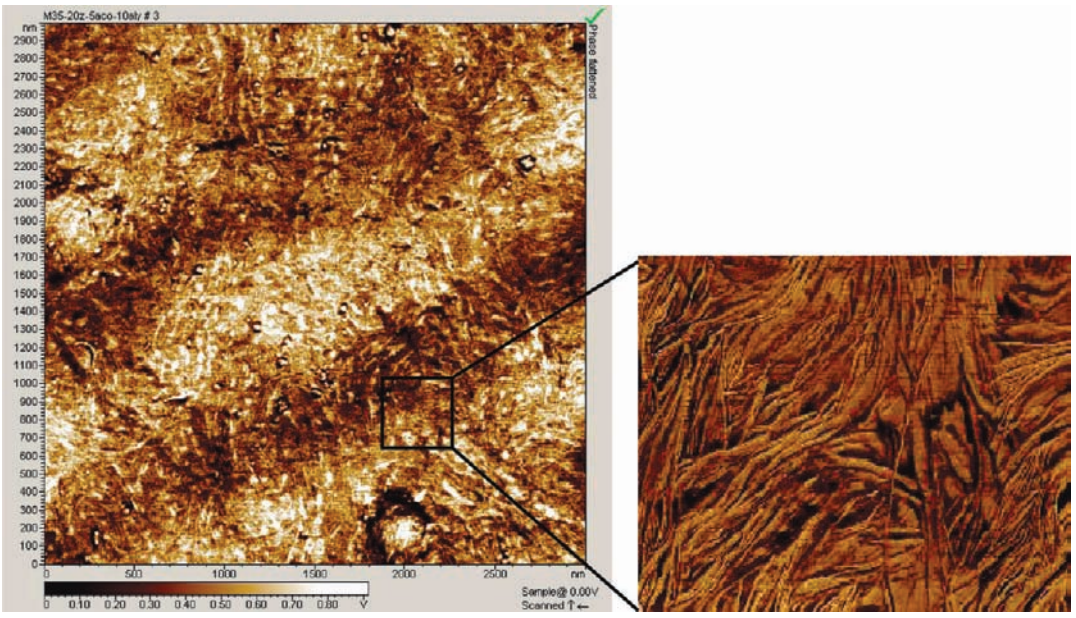

Figure 5. AFM picture of plasticized carrageenan containing 5 wt % clay and 10 wt % glycerol.

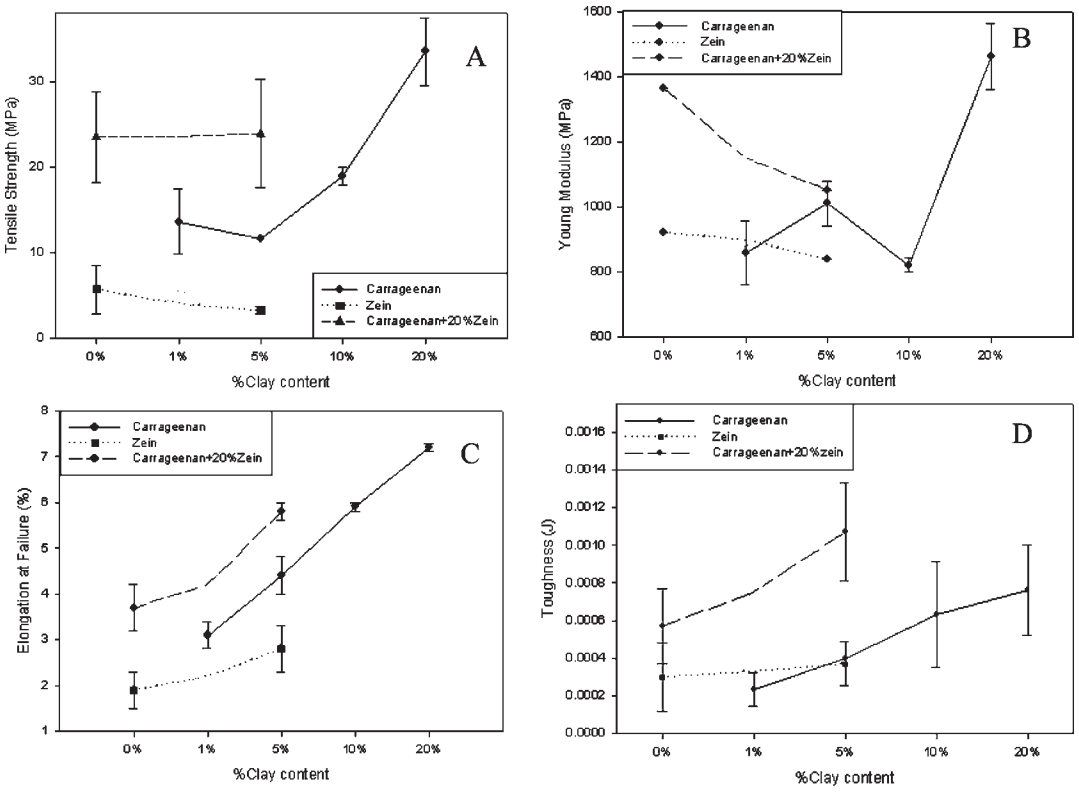

Figure 6. (A) Tensile strength (MPa), (B) Young's modulus E (MPa), (C) elongation at failure (%), and (D) toughness (J) as a function of the nanoclay content (wt %) for carrageenan, zein, and blends of carrageenan−zein.

Young's modulus of 70% for the film of carrageenan with 20 wt % nanoclay compared to carrageenan with 1 wt % content was observed. The addition of zein to the carrageenan seemed to increase Young's modulus in agreement with the above cited previous work (*20*). However, the rigidity of the nanocomposites of this blend was reduced with an increasing clay content, similar to the composites of zein.

Elongation at failure for these biopolymers and their nanocomposites is presented in **Figure 6C**. For pure carrageenan, an increase of up to 132% for the film of carrageenan with 20 wt % nanoclay compared to carrageenan with 1 wt % content can be observed. Elongation at failure was seen to increase in all cases in accordance with previous works (*27*, *28*). Toughness was, in accordance with the above, seen to increase with the presence and content of clay in the biopolymers (see **Figure 6D**). This is a very positive finding from an applied viewpoint because the extreme rigidity of these biomaterials restrict its usability to a considerable extent.

In summary, tensile strength, Young's modulus, elongation at failure, and toughness increased with an increasing clay loading in

Table 1. Water Permeability, Water Uptake (%) at 11, 54, and 75% RH for Carrageenan and Carrageenan−Zein Films and Their Nanocomposites

	water permeability (kg m^{-1} s^{-1} Pa^{-1})	water uptake (%) at 11% RH	water uptake (%) at 54% RH	water uptake (%) at 75% RH
carrageenan	$6.86 \pm 0.041 \times 10^{-14}$	5.12	10.90 ± 0.29	17.02 ± 0.34
carrageenan + 5% clay	$4.74 \pm 0.023 \times 10^{-14}$	4.99 ± 0.38	9.44 ± 0.34	16.35 ± 0.43
carrageenan + 10% glycerol	$4.65 \pm 0.542 \times 10^{-14}$	3.62 ± 0.32	12.41	26.03 ± 0.62
carrageenan + 1% clay + 10% glycerol	$0.65 \pm 0.19 \times 10^{-14}$	3.71 ± 1.26	1.84 ± 2.72	11.35 ± 1.64
carrageenan + 5% clay + 10% glycerol	$0.81 \pm 0.52 \times 10^{-14}$	5.57	1.21	11.36 ± 0.29
carrageenan + 10% clay + 10% glycerol	$1.82 \pm 0.35 \times 10^{-14}$	5.28 ± 1.33	2.39 ± 0.07	10.18 ± 1.05
carrageenan + 20% clay + 10% glycerol	$1.80 \pm 0.03 \times 10^{-14}$	7.75 ± 4.37	4.79 ± 0.62	9.21 ± 0.20
carrageenan + 20% zein + 10% glycerol	$5.65 \pm 0.248 \times 10^{-14}$	3.06 ± 0.29	8.66 ± 0.29	21.14 ± 0.98
carrageenan + 20% zein + 5% clay + 10% glycerol	$3.81 \pm 0.056 \times 10^{-14}$	1.44 ± 0.39	7.55 ± 0.52	17.42
zein + 10% glycerol		1.68	3.74 ± 0.57	9.77 ± 0.80
zein + 5% clay + 10% glycerol		1.67 ± 0.25	3.61 ± 0.54	6.04 ± 0.511
zein + 25% glycerol	7.41×10^{-14}	1.22 ± 0.16	4.83 ± 0.70	13.39 ± 0.52
zein + 5% clay + 25% glycerol	$7.71 \pm 0.776 \times 10^{-14}$	2.39	5.99 ± 0.72	9.37
κ/ι-hybrid carrageenan literature value (*4*)	6.7×10^{-14}			
zein literature value (*34*)	30.36×10^{-14}			
zein literature value (*35*)	53.50×10^{-14}			

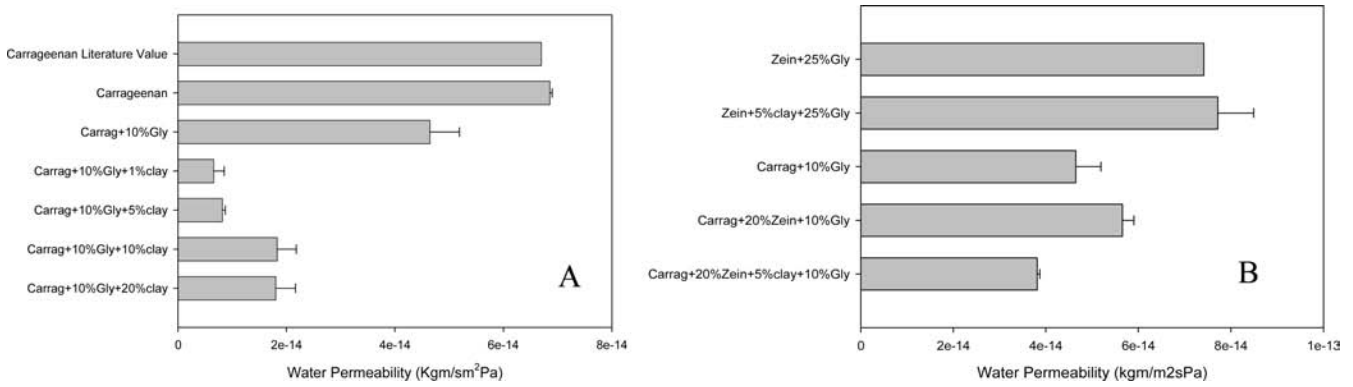

Figure 7. Water direct permeability for (A) films of carrageenan and their nanocomposites and (B) films of carrageenan/zein blends and their nanocomposites.

the case of carrageenan because of the good dispersion of the clays in the carrageenan. However, in the case of the nanocomposites of carrageenan−zein, the rigidity was not enhanced, possibly because of phase separation, the very different mechanical response of the two biopolymers, and the lower affinity of the zein for the nanoclay.

3.3. Barrier Properties. Table 1 gathers all of the barrier data (direct permeability and solvent uptake) that has been measured in the neat biopolymers and in their biocomposites and also gathers permeability values reported in the literature for the neat biopolymers.

The first observation from **Table 1** regarding pure carrageenan is that the water permeability coefficient of 6.86×10^{-14} kg m^{-1} s^{-1} Pa^{-1} is really similar to the literature value of 6.7×10^{-14} kg m^{-1} s^{-1} Pa^{-1} previously reported for this κ/ι-hybrid carrageenan (*4*). An interesting observation is the effect of glycerol in the barrier properties; **Table 1** indicates that the water permeability decreased by ca. 32% with the addition of 10 wt % glycerol, as expected for low additions of glycerol to the matrix. Talja et al. reported that the water permeability of potato starch-based films was higher without a plasticizer than with 20 wt % glycerol at all RH gradients. However, the films plasticized with 30 or 40 wt % glycerol exhibited increased water permeability (*16*). The increase in water permeability for plasticizer-free potato starch-based films was attributed by the authors to the presence of microcracks in the pure biopolymer film. The carrageenan samples studied here did not show evidence of microcracks upon careful inspection. Guo et al. also reported that cellulose acetate films with plasticizer contents of 5−10 wt % (w/w, solids) had lower water permeability than films without a plasticizer. They attributed this behavior to a decreased molecular mobility of cellulose acetate in the presence of plasticizers (*32*).

Table 1 and **Figure 7A** teach that the water permeability shows a minimum value for specimens containing 1 and 5 wt % nanoclay. From the results, a decrease in the water permeability of ca. 86, 83, 61, and 61% for the films of plasticized carrageenan containing 1, 5, 10, and 20 wt % clay, respectively, were seen compared to the unfilled plasticized material. Therefore, the addition of the clays to the plasticized carrageenan films considerably enhances the water barrier properties. Nevertheless, the addition of higher nanoclay contents (10 and 20 wt % clay) results in lower reductions in water permeability, most likely because of nanoclay agglomeration, which results in a reduction in the nanoclay barrier efficiency as a result of the creation of preferential paths for diffusion. These results are not in coincidence with a recent paper that used the same type of mica-based nanoclay but in methyl cellulose and chitosan (*13*). In the latter materials, higher loadings of clay, i.e., 20 wt %, were needed to achieve similar water permeability reductions; however, these materials did not make use of glycerol as a plasticizer. From the morphology results reported above, glycerol enhances the nanoclay dispersion in carrageenan. In fact, **Table 1** indicates that, if 5 wt % nanoclay is added to carrageenan without glycerol, the permeability reduction is smaller, i.e., 31% in permeability drop, suggesting that the dispersion is indeed poorer.

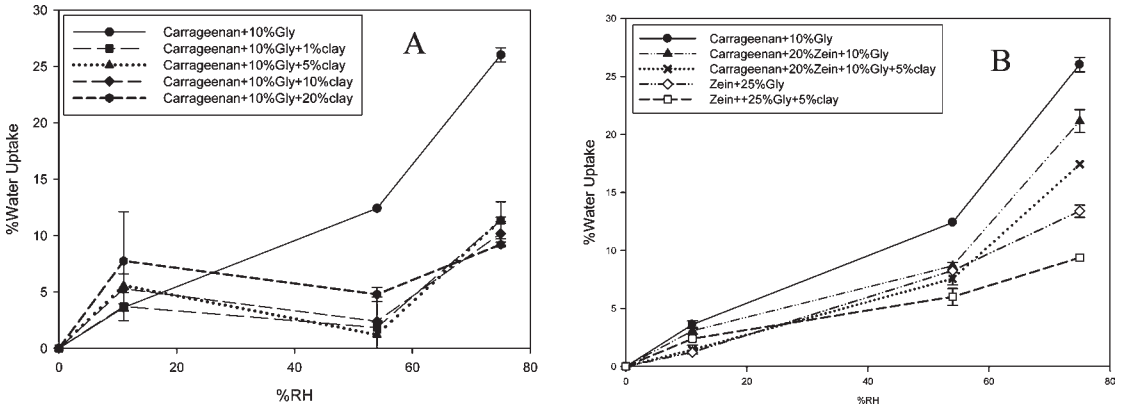

Figure 8. Water uptake (%) at 11, 54, and 75% RH for (A) films of carrageenan and their nanocomposites and (B) films of carrageenan and zein and their nanocomposites.

The water uptake of the carrageenan films and their related nanobiocomposites at different humidities is also summarized in **Table 1**. A general observation is that the water uptake increased for all samples with an increasing RH, as expected (*16*). Also, the presence of glycerol increased the water uptake but only at a medium−high percentage of RH. The uptake was higher at a higher percentage of RH. The same behavior was reported by Zeppa et al. (*33*). Thus, glycerol was seen to decrease the water uptake at low activity but increased it at high activity. This phenomenon has been attributed to potential interactions between the hydroxyl groups of carrageenan and the hydroxyl groups of glycerol, resulting in less sorption sites for water molecules (*16*, *33*).

Interestingly, the films of plasticized carrageenan containing 1, 5, 10, and 20 wt % clay exhibited clearly lower uptakes at 75% RH, i.e., ca. 56, 56, 61, and 65%, respectively, compared to the unfilled plasticized material. At 54% RH, higher reductions of 85, 90, 81, and 61% were observed with increasing clay content (see **Figure 8A**). However, at 11% RH, the nanocomposites took up more moisture than the unfilled material, most likely by moisture being preferentially sorbed at the nanoclay surface. The significantly lower water uptake at medium−high RH but especially at medium RH must be related to a water solubility reduction because of the presence of the nanoclays filling the available free volume in the biopolymer matrix as moisture begins to plasticize the biopolymer.

Tabla **2** and **Figure 7B** also show the water permeability of plasticized zein films. A first observation is that the water permeability of zein containing 25 wt % glycerol is 7.41×10^{-14} kg m^{-1} s^{-1} Pa^{-1}, whereas a film of pure zein was reported by Parris et al. to be of 30.34×10^{-14} kg m^{-1} s^{-1} Pa^{-1} (*34*) and by Ghanbarzadeh et al. to be of 53.50×10^{-14} kg m^{-1} s^{-1} Pa^{-1} in a compression-molded zein film (*35*). The reason for the disagreement could be related to the different origin, testing conditions, composition, and processing of the films. From the results, the water permeability of the plasticized zein film is seen higher than the water permeability of the pure plasticized carrageenan. Moreover, the addition of zein to carrageenan in the presence of glycerol did not outperform in the barrier properties of plasticized carrageenan. However, the nanocomposites of carrageenan−zein show a reduction in the water permeability of 18% compared to the plasticized carrageenan. Hence, the nanoclay seems a more efficient element than zein to reduce the water permeability of carrageenan.

In terms of the water uptake of zein (see **Figure 8B**), it is observed that the water resistance in terms of uptake of the polymer is much higher than that of carrageenan, as expected.

Table 2. UV−Vis Blocking (% $T_{nanocomposite}$ − % $T_{pristine}$) at 300 nm (UV) and 600 nm (Vis) Wavelengths per Weight Percent Nanoclay in Plasticized Carrageenan Nanocomposites

wt % filler	blocking at 300 nm (% *T*/wt % clay)	blocking at 600 nm (% *T*/wt % clay)
1	0	21.26
5	8.92	8.06
10	4.14	7.45
20	2.19	4.03

Thus, the water uptake of zein containing 25 wt % glycerol measured at 11, 54, and 75% RH is 66, 61, and 48%, respectively, smaller than plasticized carrageenan. In good accordance, blends of carrageenan containing 20 wt % zein show a reduction in the water uptake of 15, 30, and 19%, respectively, compared to plasticized carrageenan. Again, in the case of the nanocomposites of the blend, a reduction in the water uptake at 11, 54, and 75% RH of ca. 60, 40, and 33%, respectively, were seen compared to the plasticized carrageenan films.

Nielsen (*36*) developed an expression to model the permeability of a two-phase film in which impermeable square plates are dispersed in a continuous conducting matrix. The plates are oriented so that the two edges of equal length, L, are perpendicular to the direction of transport and the third edge, the thickness W, is parallel to the direction of transport. This expression is

$$P = P_m(1-\phi_d)/[1+(L/2W)\phi_d] \quad (1)$$

where P is the permeability of the composite, P_m, is the permeability of the matrix, and Φ_d is the volume fraction of the impermeable filler. The $(1 - \Phi_d)$ term accounts for volume exclusion, and the $(1 + (L/2W)\Phi_d)$ term accounts for tortuosity. Note that this model does not account for permeation through the dispersed phase.

A more realistic system to consider is one in which a discontinuous low-permeability phase is present in a high-permeability matrix. Maxwell (*37*) developed a model to describe the conductivity of a two-phase system in which permeable spheres are dispersed in a continuous permeable matrix. Fricke (*38*) extended Maxwell's model to describe the conductivity of a two-phase system in which permeable ellipsoids are dispersed in a more permeable continuous matrix. This model describes the permeability of a two-phase system in which lower permeability elongated ellipsoids (P_d) are dispersed in a more permeable continuous matrix (P_m).

According to the latter model, the permeability of a composite system consisting of a blend of the two materials in which the

dispersed phase (Φ_2 is the volume fraction of the dispersed phase) is distributed as ellipsoids can be expressed as follows (*39*):

$$P = (P_m + P_d F)/(1 + F) \quad (2)$$

where

$$F = [\Phi_2/1 - \Phi_2][1/(1 + (1 - M)(P_d/P_m - 1))] \quad (3)$$

$$M = \cos\theta/\sin^3\theta[\theta - 1/2 \sin 2\theta] \quad (4)$$

and

$$\cos\theta = W/L \quad (5)$$

where $\rho_{clay} = 2.7$ g/mL, $P_d \approx 0$, $P_m = 100$, and L/W was taken as 8 and 100.

W is the dimension of the axis of the ellipsoid parallel to the direction of transport, and L the dimension perpendicular to the direction of transport. θ is given in radians.

Figure 9 shows the experimental permeability values for the plasticized carrageenan system and modeling results using the Nielsen model and Fricke extended Maxwell's models. The Fricke modeling results for the higher aspect ratios best fit the data at lower filler volumes (between 1 and 5 wt % clay).

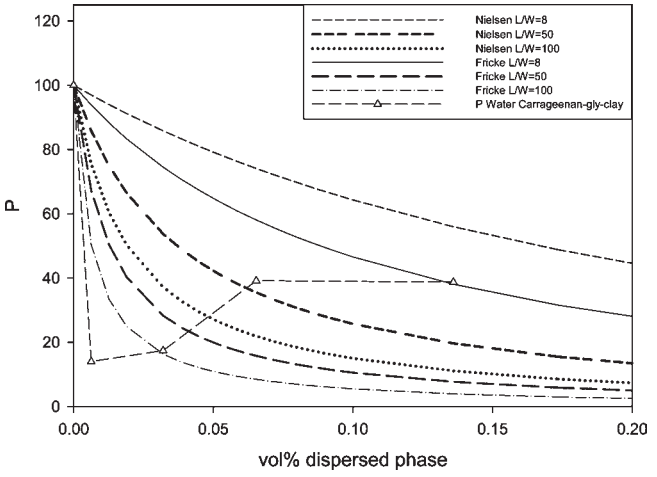

Figure 9. Experimental normalized permeability values and modeling results assuming different aspect ratios.

However, higher clay loading contents (between 10 and 20 wt % clay) do not follow the modeling trend, suggesting as explained above that agglomeration of the nanoclay decreases the barrier efficiency.

3.4. UV−Vis. Figure 10 shows the visual appearance of the plasticized carrageenan composite films. From this figure, an increase in coloring of the sample and a reduction in transparency was observed with increasing clay content, particularly for the sample containing 20 wt % filler. Nevertheless, low filler contents still exhibit good contact transparency.

Figure 11 shows the normalized transmittance for the UV−vis spectra of the nanocomposite films of plasticized carrageenan with 30 μm thickness. The UV region is typically classified in three zones: UVC (ultraviolet C) (100−280 nm), UVB (ultraviolet B) (280−320 nm), and UVA (ultraviolet A) (320−400 nm).

From **Figure 11**, a clear reduction in UV−vis transmittance with increasing clay content in the films was observed. From the results, the transmittance of the pure carrageenan in the region of UVC is around 30%. A complete shielding of UVC occurs for the selected thickness at 10 and 20 wt % clay loading in the carrageenan film. Films of carrageenan containing 20 wt % nanoclay led to reductions in the transmission of light in the UVB−UVA of ca. 95−100%. In the visible region, pure

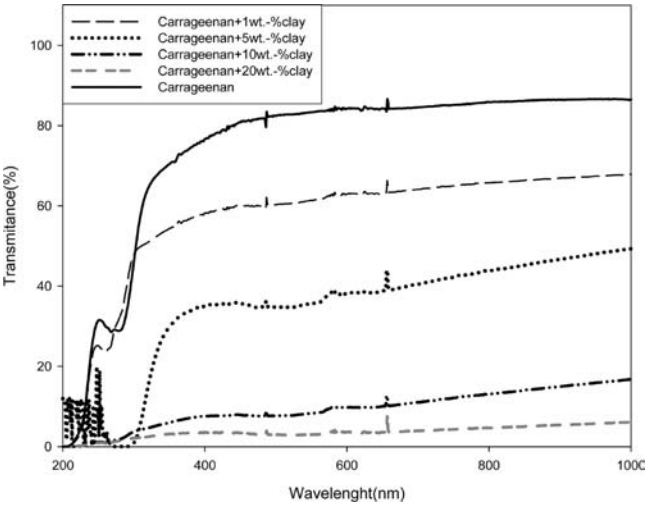

Figure 11. UV−vis spectra of 30 μm films of plasticized carrageenan nanocomposites containing 0, 1, 5, 10, and 20 wt % nanoclay.

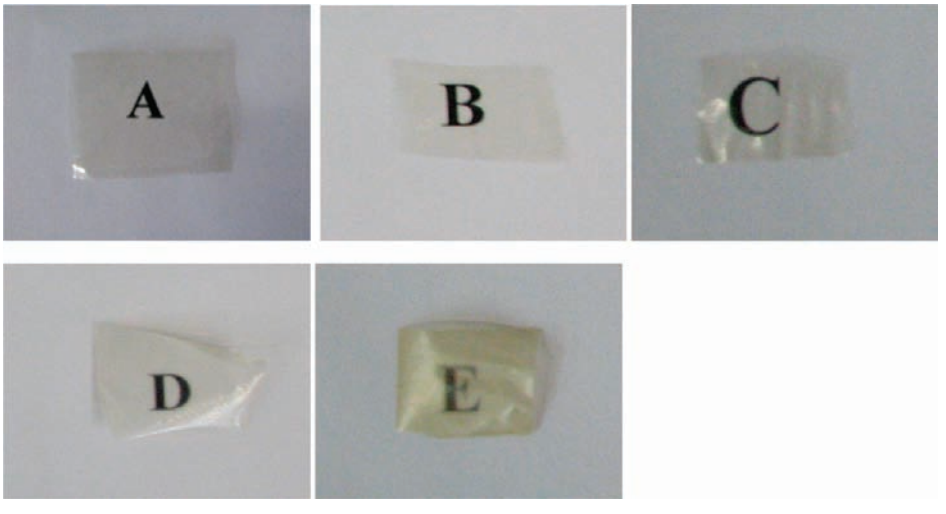

Figure 10. Typical photographs of ca. 30 μm thickness films of plasticized carrageenan containing: (A) 0 wt % clay, (B) 1 wt % clay, (C) 5 wt % clay, (D) 10 wt % clay, and (E) 20 wt % clay.

plasticized carrageenan has a transmittance of 85%, whereas the film of plasticized carrageenan containing 20 wt % clay has very little transmittance.

It is clear that 20 wt % filler loading is perhaps too high of a loading because it does negatively affect the transmission in the visible range and will be unlikely to yield an optimum property balance. Nevertheless and as observed with the barrier performance, the ratio of protection is still very efficient at nanoclay loadings of 5 wt %, yielding the 10 wt % filler not so strong differentiating benefits. Thus, low nanoclay contents (5 wt %) in the carrageenan matrix led to significant reductions in the UV light transmission (see **Table 2**) while retaining transparency to a significant extent.

In conclusion, successful blends of carrageenan with zein prolamine and a mica clay additive were obtained by solution casting using glycerol as a plasticizer. From the results, the addition of glycerol to the carrageenan nanocomposite films permitted us to obtain a good dispersed morphology of the inorganic additive, especially at low filler contents. The addition of zein to the plasticized carrageenan films showed phase separation but with strong adhesion, suggesting that the two polymers are not miscible but are compatible. Tensile strength, Young's modulus, elongation at failure, and toughness increased with increasing clay loading for the plasticized carrageenan composites, because of the good dispersion of the clays in the matrix. However, for the carrageenan−zein composites, the rigidity was not enhanced, possibly because of the mentioned phase separation, the very different mechanical response of the two biopolymers, and the lower affinity of the zein for the nanoclay. Interestingly, the addition of nanoclays (1 or 5 wt %) to the plasticized carrageenan decreased the water permeability significantly by ca. 86 and 83%, respectively. The water uptake was also reduced by up to ca. 90% in samples with low nanoclay contents at high RH, suggesting that the observed lower water permeability may be strongly contributed by a nanoclay-induced solubility drop effect. Additionally, low nanoclay contents (1 or 5 wt %) in the carrageenan matrix led to significant reductions in the UV−vis light transmission while retaining transparency. These results suggest that these blends can have significant potential in food packaging and coating applications, where enhanced water resistance and permeability and increased flexibility can provide more usability for the polysaccharide.

ACKNOWLEDGMENT

Dr. E. Gimenez from the Universidad Politécnica de Valencia (UPV), Valencia, Spain, is acknowledged for support with the mechanical testing.

LITERATURE CITED

(1) Hilliou, L.; Larotonda, F. D. S.; Abreu, P.; Ramos, A. M.; Sereno, A. M.; Gonçalves, M. P. Effect of extraction parameters on the chemical structure and gel properties of κ/ι-hybrid carrageenans obtained from *Mastocarpus stellatus*. *Biomol. Eng.* **2006**, *23*, 201–208.

(2) Hilliou, L.; Larotonda, F. D. S.; Sereno, A. M.; Gonçalves, M. P. Thermal and viscoelastic properties of κ/ι-hybrid carrageenan gels obtained from the Portuguese seaweed *Mastocarpus stellatus*. *J. Agric. Food Chem.* **2006**, *54* (20), 7870–7878.

(3) Hilliou, L.; Gonçalves, M. P. Gelling properties of a κ/ι-hybrid carrageenan: Effect of concentration and steady shear. *Int. J. Food Sci. Technol.* **2007**, *42*, 678–685.

(4) Larontonda, F. D. S.; Hilliou, L.; Goncalves, M. P.; Sereno, A. M. From low value renewable resources to green biomaterials for edible coating applications. In *Recent Advances In Research on Biodegradable Polymers and Sustainable Composites*; Jiménez, A., Zaikoz, G. E., Eds.; Nova Science Publishers, Inc.: Hauppauge, NY, 2008; Vol. 3, p 19, ISBN 978-1-60692-155-5.

(5) De Ruiter, G. A.; Rudolph, B. Carrageenan biotechnology. *Trends Food Sci. Technol.* **1997**, *8*, 389–395.

(6) Shaw, C.; Secrist, J.; Tuomy, J. Method of extending the storage life in the frozen state of precooked foods and product produced. U.S. Patent 4,196,219, 1980.

(7) Macquarrie, R. Edible film formulation. U.S. Patent 0155200 A1, 2002.

(8) Ninomiya, H.; Suzuki, S.; Ishii, K. Edible film and method of making same. U.S. Patent 5,620,757, 1997.

(9) Tanner, K.; Getz, J.; Burnett, S.; Youngblood, E.; Draper, P. Film forming compositions comprising modified starches and ι-carrageenan and methods for manufacturing soft capsules using same. U.S. Patent 0081331 A1, 2002.

(10) Bartkowiak, A.; Hunkeler, D. Carrageenan−oligochitosan microcapsules: Optimization of the formation process. *Colloids Surf., B* **2001**, *21*, 285–298.

(11) Fonkwe, L.; Archibald, D.; Gennadios, A. Nongelatin capsule shell formulation. U.S. Patent 0138482 A1, 2003.

(12) Brody, A. L. Edible packaging. *Food Technol.* **2005**, *59*, 65.

(13) Lagaron, J. M.; Fendler, A. High water barrier nanobiocomposites of methyl cellulose and chitosan for film and coating applications. *J. Plast. Film Sheeting* **2009**, *25* (1), 47–59.

(14) Tihminlioglu, F.; Atik, I. D.; Özen, B. Water vapor and oxygen-barrier performance of corn−zein coated polypropylene films. *J. Food Eng.* **2010**, *96*, 342–347.

(15) Guilbert, S.; Gontard, N.; Gorris, L. G. M. Prolongation of the shelflife of perishable food products using biodegradable films and coatings. *LWT—Food Sci. Technol.* **1996**, *29*, 10–17.

(16) Talja, R. A.; Helén, H.; Roos, Y. H.; Jouppila, K. Effect of various polyols and polyol contents on physical and mechanical properties of potato starch-based films. *Carbohydr. Polym.* **2007**, *67*, 288–295.

(17) Schou, M.; Longares, A.; Montesinos-Herrero, C.; Monahan, F. J.; O'Riordan, D.; O'Sullivan, M. Properties of edible sodium caseinate films and their application as food wrapping. *LWT—Food Sci. Technol.* **2005**, *38*, 605–610.

(18) Padua, G. W.; Rakoronirainy, A.; Wang, Q. Zein-based biodegradable packaging for frozen foods. Proceedings of the the Food Biopack Conference, Copenhagen, Denmark, Aug 27−29, **2000**; pp 84−88.

(19) Arora, A.; Pádua, G. W. Review: Nanocomposites in food packaging. *J. Food Sci.* **2010**, *75* (1), R43–R49.

(20) Kim, S. Processing and properties of gluten/zein composite. *Bioresour. Technol.* **2008**, *99*, 2032–2036.

(21) Corradini, E.; De Medeiros, E. S.; Carvalho, A. J. F.; Curvelo, A. A. S.; Mattoso, L. H. C. Mechanical and morphological characterization of starch/zein blends plasticized with glycerol. *J. Appl. Polym. Sci.* **2006**, *101*, 4133–4139.

(22) Pol, H.; Dawson, P.; Acton, J.; Ogale, A. Soy protein isolate/corn−zein laminated films: Transport and mechanical properties. *J. Food Sci.* **2002**, No. 1, 67–217.

(23) Corradini, E.; de Carvalho, A. J. F.; Curvelo, A. A.; da, S.; Agnelli, J. A. M.; Mattoso, L. H. C. Preparation and characterization of thermoplastic starch/zein blends. *Mater. Res.* **2007**, *10* (3), 227–231.

(24) Daniel-Da-Silva, A. L.; Lopes, A. B.; Gil, A. M.; Correia, R. N. Synthesis and characterization of porous κ-carrageenan/calcium phosphate nanocomposite scaffolds. *J. Mater. Sci.* **2007**, *42*, 8581–8591.

(25) Gan, S.-L.; Feng, Q.-L. Preparation and characterization of a new injectable bone substitute-carrageenan/nano-hydroxyapatite/collagen. *Acta Acad. Med. Sin.* **2006**, *28* (5), 710–713.

(26) Olabarrieta, I.; Gällstedt, M.; Ispizua, I.; Sarasua, J. R.; Hedenqvist, M. S. Properties of aged montmorillonite−wheat gluten composite films. *J. Agric. Food Chem.* **2006**, *54*, 1283–1288.

(27) Wang, N.; Zhang, X.; Han, N.; Bai, S. Effect of citric acid and processing on the performance of thermoplastic starch/montmorillonite nanocomposites. *Carbohydr. Polym.* **2009**, *76*, 68–73.

(28) Chang, J.-H.; Uk-An, Y.; Sur, G. S. Poly(lactic acid) nanocomposites with various organoclays. I. thermomechanical properties, morphology, and gas permeability. *J. Polym. Sci., Part B: Polym. Phys.* **2003**, *41*, 94–103.

(29) Majdzadeh-Ardakani, K.; Navarchian, A. H.; Sadeghi, F. Optimization of mechanical properties of thermoplastic starch/clay nanocomposites. *Carbohydr. Polym.* **2010**, *79*, 547–554.
(30) Soundararajah, Q. Y.; Karunaratne, B. S. B.; Rajapakse, R. M. G. Montmorillonite polyaniline nanocomposites: Preparation, characterization and investigation of mechanical properties. *Mater. Chem. Phys.* **2009**, *113*, 850–855.
(31) Ganguly, A.; Bhowmick, A. K. Effect of polar modification on morphology and properties of styrene-(ethylene-co-butylene)-styrene triblock copolymer and its montmorillonite clay-based nanocomposites. *Mater. Sci.* **2009**, *44*, 903–918.
(32) Guo, J. H. Effects of plasticizers on water permeation and mechanical properties of cellulose acetate: Antiplasticization in slightly plasticized polymer film. *Drug Dev. Ind. Pharm.* **1993**, *19* (13), 1541–1555.
(33) Zeppa, C.; Gouanve, F.; Espuche, E. Effect of a plasticizer on the structure of biodegradable starch/clay nanocomposites: Thermal, water-sorption, and oxygen-barrier properties. *J. Appl. Polym. Sci.* **2009**, *112*, 2044–2056.
(34) Parris, N.; Dickey, L. C.; Kurantz, M. J.; Moten, R. O.; Craig, J. C. Water vapor permeability and solubility of zein/starch hydrophilic films prepared from dry milled corn extract. *J. Food Eng.* **1997**, *32* (2), 199–207.
(35) Ghanbarzadeh, B.; Musavi, M.; Oromiehie, A. R.; Rezayi, K.; Razmi Rad, E.; Milani, J. Effect of plasticizing sugars on water vapor permeability, surface energy and microstructure properties of zein films. *Food Sci. Technol.* **2007**, *40* (7), 1191–1197.
(36) Nielsen, L. W. Models for the permeability of filledpolymer systems. *J. Macromol. Sci.* **1967**, *Al*, 929.
(37) Maxwell, J. C. *Electricity and Magnetism*, 3rd ed.; Dover Publications, Inc.: New York, 1891; Vol. 1.
(38) Fricke, H. A mathematical treatment of the electric conductivity and capacity of disperse systems. I. The electric conductivity of a suspension of homogeneous spheroids. *Phys. Rev.* **1924**, *24*, 575.
(39) Paul, D. R.; Bucknall, C. B. *Polymer Blends*; Wiley-Interscience: New York, 2000; Vol. 2, Performance.

Received for review February 24, 2010. Revised manuscript received April 19, 2010. Accepted April 27, 2010. The authors thank the MICINN projects MAT2009-14533-C02-01 and EUI2008-00182 and projects POCTI/EQU/45595/2002 and POCI/EQU/58064/2004 for financial support. M.D.S.-G. thanks the FPI program of the GV associated with the MEC project MAT2003-08480-C3 for the research grant.